Photon Correlations from the Mollow Triplet

Juan Camilo López Carreño, Elena del Valle, and Fabrice P. Laussy*

Abstract: Photon correlations between the photoluminescence peaks of the Mollow triplet have been known for a long time, and recently hailed as a resource for heralded single-photon sources. Here, we provide the full picture of photon-correlations at all orders (we deal explicitly with up to four photons) and with no restriction to the peculiar frequency windows that enclose the peaks. We show that a rich multi-photon physics lies between the peaks, due to transitions involving virtual photons, and thereby much more strongly correlated than those transiting through the real states. Specifically, we show that such emissions occur in bundles of photons rather than as successive, albeit correlated, photons. We provide the recipe to frequency-filter the emission of the Mollow triplet to turn it into a versatile and tunable photon source, allowing in principle all scenarios of photon emission, with advantages already at the one-photon level, i.e., providing more strongly correlated heralded single-photon sources than those already known.

1. Introduction

Resonance fluorescence is one of the simplest and yet most fruitful cases of light-matter interaction. It describes the emission of a two-level system (2LS) that is driven coherently and at the same frequency than it emits.[1] Following the prediction of its antibunching emission,[2] it provided the first direct evidence of quantization of the light field[3] (the photo-electric effect, that suggests it, could also be explained semi-classically). The interferences between the absorbed and emitted light result in counter-intuitive effects[4,5] that power one of the best mechanisms for single-photon emission, currently under fervent development.[6] Of particular interest is the high excitation regime, described theoretically by Benjamin Mollow in 1969[7] and first observed by crossing at right angle a low-density gas of sodium atoms with a dye laser beam at resonance with a two-level Na transition (the $F = 2 \rightarrow 3$ hyper-fine transition of the D_2 line),[8] an observation since then repeated in a wealth of other platforms.[9–18] The appeal

of this high-driving fluorescence comes from its peculiar spectral lineshape, that takes the form of a triplet (shown in **Fig. 1**).

The most elegant physical interpretation of this triplet describes the 2LS as dressed by the laser.[19,20] This gives rise to new eigenstates $|\pm\rangle$, formed from a combination of bare states $|g, n+1\rangle$ and $|e, n\rangle$, where "g", "e" correspond to the "ground" and "excited" states of the 2LS, respectively, and n to the (integer) number of photons from the laser. A family of such states whose total energy is the same, forms a so-called "manifold of excitation" (this used to be called a "multiplicity" but the term "manifold" is nowadays more common). In every manifold, the eigenstates are split by the Rabi frequency, while the energy difference between two contiguous manifolds is that of the bare states, (or their average if not resonant), as shown in Fig. 1, which displays five manifolds. The transitions between contiguous manifolds account for the main features: a triplet in which the integrated spectral intensities of its peaks have 1:2:1 proportions (when the laser is resonant with the 2LS). The properties of the underlying states $|\pm\rangle$ have been studied early on, with a good quantitative description from the dressed state picture. Apanasevich and Kilin[21] first computed in this framework the photon correlations between the peaks and predicted most of their qualitative cross-correlations, such as antibunching for each side-peak emission and bunching between them. Following similar (and independent) theoretical predictions from Cohen Tannoudji and Reynaud,[22] Aspect *et al.*[23] measured such photon correlations between the side peaks, confirming the radiative cascade and time-ordering so naturally explained by the dressed atom picture.[24] Schrama *et al.*[25,26] extended the theory to the regime of small correlation times, which requires to take into account interferences between the various emitted photons, resulting for instance in antibunching between a side-peak and a central-peak photons instead of uncorrelated emission as suggested by the earlier theories. They obtained excellent quantitative agreement with correlations measured from the resonance fluorescence of the $^1S_0 \rightarrow {}^1P_1$ transition in barium, albeit after several types of corrections to take into account experimental limitations. This has remained the state of the art until the recent re-emergence of this problem in the solid state, with Ulhaq *et al.*[27]'s revisiting of the photon correlations between the peaks from the resonance fluorescence of an In(Ga)As quantum dot. A more recent work brought the two platforms together in an hybrid setup where the quantum dot is filtered by the Faraday anomalous dispersion of a cesium atom.[28] In these and previous experiments as well as in the bulk of the

Juan Camilo López Carreño, Elena del Valle
Departamento de Física Teórica de la Materia Condensada
Universidad Autónoma de Madrid,
28049, Madrid, Spain

Juan Camilo López Carreño, Fabrice P. Laussy
Faculty of Science and Engineering
University of Wolverhampton
Wulfruna St, Wolverhampton, WV1 1LY, UK
E-mail: F.Laussy@wlv.ac.uk

Fabrice P. Laussy
Russian Quantum Center
Novaya 100, 143025, Skolkovo, Moscow Region, Russia

**ADVANCED
SCIENCE NEWS**

www.advancedsciencenews.com

LASER
& PHOTONICS
REVIEWS

www.lpr-journal.org
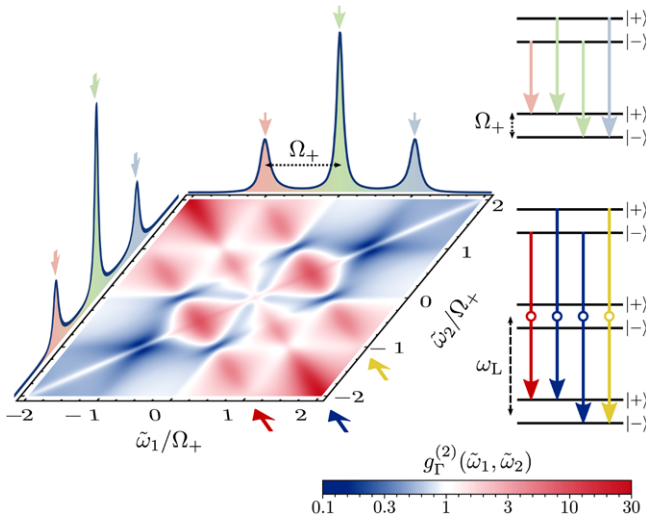
Figure 1. (Color online). The Mollow triplet (spectral lineshape) and its two-photon spectrum that correlates all the combinations of frequencies (density plot) with the ladder of dressed states (right) whose transitions between manifolds account for the main phenomenology: the power spectrum at the one-photon level and resonances in the two-photon spectrum. The manifestations in the two types of spectra of the one- and two-photon transitions in the ladder are indicated by arrows of corresponding colors. Of particular interest, the two-photon "leapfrog processes" indicated by the red, blue and yellow arrows give rise to strong bunching antidiagonals in the density plot. The results were obtained by driving the 2LS resonantly with the laser pumping rate $\Omega = 5\gamma_\sigma$ and filtering the emission with a detector of linewidth $\Gamma = \gamma_\sigma$ where γ_σ (the decay rate of the 2LS) sets the unit. The Rabi frequency, Ω_+, gives the splitting in each manifold and correspondingly, the position of the side peaks of the Mollow triplet. The energy of one laser-photon, ω_L, is taken as a reference for the variables $\tilde\omega_k \equiv \omega_k - \omega_L$. The color code throughout the text is red for $g_\Gamma^{(2)} > 1$, white for $g_\Gamma^{(2)} = 1$ and blue for $g_\Gamma^{(2)} < 1$, with the deepest red (blue) set to the maximum (minimum) value.

theoretical efforts, the photon correlations have thus been limited to photons from the peaks. Meanwhile, the formal theories of frequency-resolved photon correlations led to increasingly better but also more intricate models that involve heavy computations to accommodate all the time-orderings of the emitted photons,[29–31] in particular when expanding the correlations to higher numbers of photons,[32] and this was typically tackled through approximations relying on the dressed state picture, which also constrained the computations to the peaks.

A recent theory of frequency-resolved photon correlations[33] relaxes these restrictions and permits an exact treatment, to high photon numbers and for any spectral windows. In the most popular case of two-photon correlations, this readily provides the full landscape of all correlations between all combinations of frequencies, enclosing or not the peaks.[34,35] This two-photon correlation spectrum, shown in Fig. 1, unravels a rich structure, with another triplet of lines, this time at the two-photon level, corresponding to direct transitions from one manifold to two below, jumping over the intermediate one in a "leapfrog process", sketched in the bottom of the ladder in Fig. 1. The auxiliary photon in any of these processes is virtual (represented by ○), resulting in strong correlations of the emitted pair.[36] This two-photon spectrum has been measured by Peiris et al.,[37] confirming that

the correlations between the peaks that had been known since the early years of the Mollow triplet, were particular cases of a wider picture.

In this text, we provide an exact description of higher-order photon correlations from the Mollow triplet and propose configurations that extend the realm of possible experiments and applications that have been explored so far, replacing real-state transitions by strongly-correlated leapfrog transitions. We also review the state of the art as we introduce notations and the main formalism.

2. Spectral Shape of the Mollow Triplet

The Mollow triplet is described theoretically by the Hamiltonian (we set $\hbar = 1$ along the paper and a tilde is used, here and further, over a frequency to refer it to that of the laser, ω_L, used as a reference, i.e., $\tilde\omega_\sigma \equiv \omega_\sigma - \omega_L$)

$$H_\sigma = \tilde\omega_\sigma \sigma^\dagger \sigma + \Omega(\sigma^\dagger + \sigma), \tag{1}$$

where σ is the annihilation operator of the 2LS with free energy ω_σ, while the coherent driving is described by the real number Ω (amplitude of a classical field) and its energy ω_L (absorbed in the 2LS free energy once in the rotating frame). The dissipative character of the system is taken into account through the master equation

$$\partial_t \rho = i[\rho, H_\sigma] + \frac{\gamma_\sigma}{2}\mathcal{L}_c \rho, \tag{2}$$

where γ_σ is the 2LS decay rate and $\mathcal{L}_c \rho \equiv 2c\rho c^\dagger - c^\dagger c\rho - \rho c^\dagger c$. The system enters the strong coupling regime when new eigenvalues emerge from the liouvillian.[5] In this case, which we shall consider from now on (although not a restriction for the formalism), the spectrum involves three Lorentzians split by

$$\Omega_+ \equiv \frac{\sqrt{8\Omega_0^2 - 6\gamma_\sigma^2 + \sqrt{9\gamma_\sigma^4 + 16\Omega_0^4 - 24\gamma_\sigma^2(16\Omega^2 + \Omega_0^2)}}}{2\sqrt{3}}, \tag{3}$$

with $\Omega_0^2 \equiv 4\Omega^2 + \tilde\omega_\sigma^2$. In the limit $\Omega_0 \gg \gamma_\sigma$, the splitting is simply $\Omega_+ \approx \Omega_0$ and the two sidebands have the same spectral weight while the central one decreases with detuning from twice as large at resonance to zero when $\tilde\omega_\sigma \gg \gamma_\sigma$.

While the spectral shape is readily obtained by solving the master equation, it is better understood on physical grounds as transitions between the eigenstates $|\pm\rangle \equiv (|e, n\rangle \pm |g, n+1\rangle)/\sqrt{2}$ (at resonance) introduced earlier. For $n \gg 1$—the case of strong-driving that we will consider—the splitting between $|+\rangle$ and $|-\rangle$ does not depend appreciably on n. The level structure of an infinite ladder of manifolds, separated by the energy of the laser and each split by Ω_+, pervades the phenomenology of resonance fluorescence in the high-excitation regime. The immediate insight brought by the one-photon transitions—the central peak being twice as high because two of the four transitions are degenerate— shows that this is a powerful tool to guide one's intuition. In some regime, the dressed-atom description even becomes exact[20] and quantitative results can be obtained through rate equations for the transitions between the states. The transitions that yield the

**ADVANCED
SCIENCE NEWS**
www.advancedsciencenews.com

LASER
&PHOTONICS
REVIEWS

www.lpr-journal.org

central peak, $|\pm\rangle \rightarrow |\pm\rangle$, leave the state of the 2LS unchanged, while those that yield the side peaks, $|\pm\rangle \rightarrow |\mp\rangle$, change the state of the 2LS. As detuning changes the light-matter composition of the dressed states, it can thus be used to tune the triplet's properties and control, e.g., the time-ordering of emission.[27] Early on, it was appreciated on the basis of this picture that subsequent cascades between dressed states result in photon correlations. The basic reasoning is equally simple than for explaining the lineshape. For instance, the cascade $|+\rangle \rightarrow |+\rangle \rightarrow |+\rangle$ (id. with $-$) leads to bunching from the $|+\rangle \rightarrow |+\rangle$ transition, that corresponds to the central peak. In contrast, $|+\rangle \rightarrow |-\rangle$, that corresponds to the high-energy side peak, cannot happen twice in succession, since the final state $|-\rangle$ of the first part of the cascade is orthogonal to the initial state $|+\rangle$ of the second part, effectively blocking this path of relaxation. The same holds true for $|-\rangle \rightarrow |+\rangle$, that corresponds to the low-energy side peak, leading to antibunching for both of these frequencies. A more careful analysis is needed for paths with the same initial and final states that can take different routes through the degenerate transitions $|-\rangle \rightarrow |-\rangle$ and $|+\rangle \rightarrow |+\rangle$. This leads to interferences between their probability amplitudes that forbid the transition rather than favouring it. This is the case of $|-\rangle \rightarrow |\pm\rangle \rightarrow |+\rangle$, that corresponds to photon emission from one side peak and the central peak, which is antibunched although it would appear to occur in a cascade.[25]

3. Leapfrog Processes

Another class of transitions takes place in the same ladder, that has been overlooked until its identification in the two-photon spectrum by González Tudela et al.[34] and del Valle.[35] It consists of transitions from one real state to another but involving two photons $|+\rangle \rightrightarrows |-\rangle$, three $|+\rangle \overset{3}{\rightrightarrows} |-\rangle$ or any number, jumping over as many manifolds as required (one less than the number of photons involved). There is a strong difference between $|+\rangle \rightarrow |\pm\rangle \rightarrow |-\rangle$ (a transition that is a cascade between real states) and $|+\rangle \rightrightarrows |-\rangle$ (a leapfrog transition that involves a virtual state). In a cascade between real states, each photon is real and the first transition takes place independently from the second. The correlations are thus of a classical character: the second transition becomes more likely because the first one reached the state that allows it to take place. In the other case of a leapfrog transition, the two photons are emitted simultaneously, with stronger correlations as the joint emission is intrinsic to the process. The correlations in this case are of a quantum character, as each photon does not exist on its own but is part of a two-photon emission process.[38] This also allows to relax the conditions on the photons: their individual energies do not need to match any allowed transition, only their sum does. This provides the simple equations for the two-leapfrog processes:

$$\tilde{\omega}_1 + \tilde{\omega}_2 = 0, \tag{4a}$$

$$\tilde{\omega}_1 + \tilde{\omega}_2 = \Omega_+, \tag{4b}$$

$$\tilde{\omega}_1 + \tilde{\omega}_2 = -\Omega_+, \tag{4c}$$

where $\tilde{\omega}_i \equiv \omega_i - \omega_L$ for $i = 1, 2$. While the conditions Eqs. (4a–c) can also be satisfied by photons from real transitions, this breaks the tie by transforming the virtual photons into real ones when transiting by the intermediate manifold. This mechanism can be generalized to transitions involving N photons:

$$\tilde{\omega}_1 + \tilde{\omega}_2 + \cdots + \tilde{\omega}_N = \Delta, \quad \text{with} \quad \Delta = -\Omega_+, 0, \Omega_+. \tag{5}$$

Here as well, Eq. (5) can be met by matching real transitions, with any number from one to all the intermediate photons. The most strongly correlated case corresponds to all intermediate photons being virtual, in which case we refer to an "N-photon leapfrog", hopping over $N - 1$ intermediate manifolds.

These leapfrog processes can be singled out from the total emission by spectral filtering, to select the frequencies where the corresponding photons are expected to be emitted. As characteristic of a quantum system, the combinatorics aspect quickly becomes overriding in the description of the phenomenology. At the two-photon level, the picture is fully captured by the two-photon correlation spectrum $g^{(2)}_{\Gamma_1, \Gamma_2}(\tilde{\omega}_1, t_1; \tilde{\omega}_2, t_2)$ that measures the density of probability to detect at time t_1 one photon of frequency $\tilde{\omega}_1$ in a window of width Γ_1 and another photon at time t_2 of frequency $\tilde{\omega}_2$ in a window of width Γ_2. Spanning over all the possible combinations of frequencies provides the type and strength of correlations in a landscape of correlations,[34,35] as shown in Fig. 1 for coincidences, $t_1 = t_2$, and same filters linewidths $\Gamma \equiv \Gamma_1 = \Gamma_2$. When the conditions of Eqs. (4a–c) are fulfilled, strong correlations are observed indeed in the two-photon spectrum, as can be seen in Fig. 1 in the form of the three antidiagonal lines, indicated by the red, blue and yellow arrows. As this has been widely discussed already,[34–37,39,40] we consider directly the next order, for which the standard correlation function is that provided by Glauber for order three, namely, $g^{(3)}$.[41] With frequency filtering, this becomes $g^{(3)}_{\Gamma_1, \Gamma_2, \Gamma_3}(\tilde{\omega}_1, t_1; \tilde{\omega}_2, t_2; \tilde{\omega}_3, t_3)$. Assuming here as well the same filter linewidths Γ and coincidences, $t_1 = t_2 = t_3$, we arrive at a 3D correlation spectrum $g^{(3)}_{\Gamma}(\tilde{\omega}_1, \tilde{\omega}_2, \tilde{\omega}_3)$, a two-plane cut of which is shown in **Fig. 2** (the details of its computation are given in next Section). It is not easy to visualize a three-dimensional correlation structure, but we can nevertheless characterize it fairly comprehensively. It consists essentially of leapfrog planes of superbunching, which, following Eqs. (5), read at the three-photon level

$$\tilde{\omega}_1 + \tilde{\omega}_2 + \tilde{\omega}_3 = \Delta, \tag{6a}$$

but also, as revealed by the exact calculation, of the families of planes defined by

$$\tilde{\omega}_1 + \tilde{\omega}_2 = \Delta, \tag{6b}$$

$$\tilde{\omega}_1 + \tilde{\omega}_3 = \Delta, \tag{6c}$$

$$\tilde{\omega}_2 + \tilde{\omega}_3 = \Delta, \tag{6d}$$

where in each case Δ is one of the three combinations of initial/final states transitions, i.e., $\Delta = -\Omega_+$ (the red planes in Fig. 2(b–e)), $\Delta = 0$ (blue) and $\Delta = \Omega_+$ (yellow). The planes from Eq. (6a) are the three-photon leapfrogs where all the intermediate photons are virtual, as shown in the upper part of the dressed
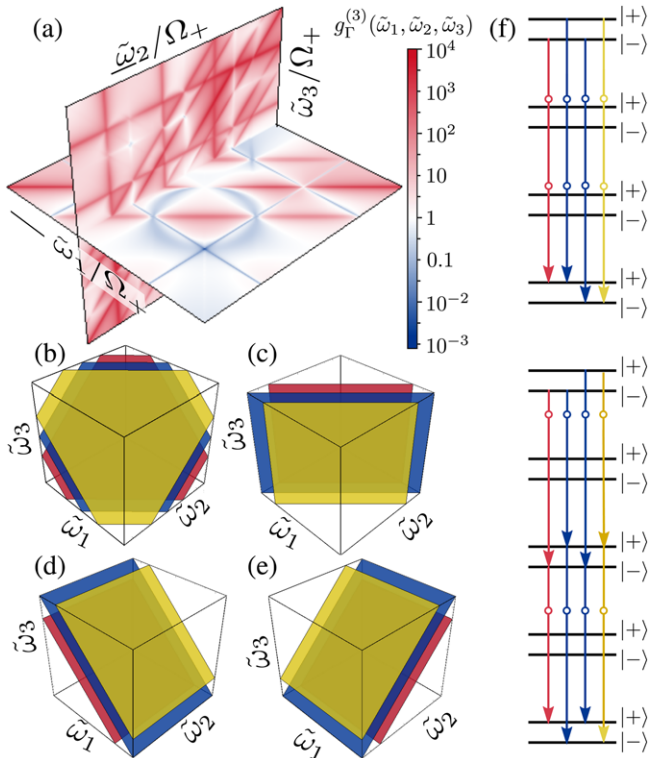
Figure 2. (Color online). High-order correlations from N-photon transitions in the Mollow triplet. (a) The 3rd-order correlation function $g_\Gamma^{(3)}(\tilde{\omega}_1, \tilde{\omega}_2, \tilde{\omega}_3)$ is shown as a two-plane cut in the full-3D structure. The vertical plane is pinned at a leapfrog transition while the horizontal plane is pinned at the central peak. The lines observed are superbunching resonances that result from the intersections with the leapfrog planes given by Eqs. (6a-d), and displayed in panels (b-e), respectively. The colors correspond to the different values of Δ, namely Ω_+ (shown in yellow), 0 (blue) and $-\Omega_+$ (red). The leapfrog transitions involved are shown in the ladder of dressed states in panel (f). At the top, the three-photon leapfrog, Eq. (6a), yield the planes shown in (b). At the bottom of the ladder, the cascades of two two-photon bundles, out of which three photons yield the planes shown in (c-e). Panel (a) was obtained for $\Omega_+ = 300\gamma_\sigma$, $\tilde{\omega}_\sigma = 200\gamma_\sigma$ and $\Gamma = 5\gamma_\sigma$, setting the decay rate γ_σ of the 2LS as the unit.

states ladder in Fig. 2(f). The planes from Eqs. (6b–d) correspond to three-photon correlations that involve two two-photon leapfrog transitions linked by a cascade, namely, with two photons belonging to one two-photon leapfrog transition while the third comes from another two-photon leapfrog transition. Alternatively, this can be seen as a four-photon leapfrog transition that intersects a real-state, breaking it in two two-leapfrog transitions. This is shown in the bottom of the ladder in Fig. 2(f). It is at this point that the concept introduced by Sánchez Muñoz et al.[36] of a "bundle"—the N-photon object issued by a leapfrog transition—becomes handy. The planes in panels (c–e) thus correspond to a bundle-bundle radiative cascade in the ladder, the same process as that discussed by Cohen-Tannoudji & Reynaud in the dressed-atom picture, but here for two-photon bundles instead of two single-photons. The planes in panel (b) correspond to a single three-photon bundle transition. The fact that four photons can team up in this way to provide correlations that appear in the three-photon spectrum $g_\Gamma^{(3)}$ is first and foremost a result of the exact computation, that can be understood in terms of leapfrog transitions, which, in turn, can make predictions that exact computations can subsequently confirm, as will be shown later on. The four-photon transitions sketched in Fig. 2(f) are the only possible ones to account for the observed leapfrog planes (c-e). If one photon would correspond to a transition between real states, we would observe lines instead of planes. A four-photon bundle on the other hand would not constrain two frequencies, as is the case of Eqs. (6b–d) and, beside, it is known that a fourth-order process is not detectable by a third-order correlator.[42] Since all the observed resonances are accounted for by the processes highlighted and that, in turn, all these processes produce a resonance in the computed correlation spectrum, the characterization of the photon correlations is indeed comprehensive. Before turning to these exact calculations, we illustrate how the powerful dressed-atom picture also allows us to make some qualitative statements on the expected behaviours at the bundle level. Specifically, let us consider degenerate N-photon bundles, i.e., with all photons having the same energy. Such bundles need to change the state of the 2LS, for otherwise they break into real-state transitions. There are therefore two types of such degenerate bundles, those with photons of frequency $-\Omega_+/N$ and those with photons of frequency Ω_+/N. Now, for the same reasons as for single photons, one can expect for two bundles of the same type to be antibunched, as the 2LS has changed state, whereas two bundles of a different type will form a cascade and can be expected to be bunched. Note that such a behaviour holds at the level of the bundles rather than at the level of the photons themselves, that should be bunched in all cases. Such "predictions" from the leapfrog picture are confirmed by exact computations.

To get a more quantitative picture, we need to turn to an exact theory of frequency-resolved three-photon correlations, that we present in next Section. Importantly, this will confirm that the leapfrog transitions in Eqs. (6a-6d) are the main three-photon relaxation processes. Every red line in Fig. 2(a) is accounted for by one of the planes in panels (b-e) of Fig. 2, and vice-versa, every plane produces a red line. This remains true for any other cuts in the 3D structure (to assist in the visualization of this three-photon correlation spectrum, we also provide an animated version as Supplementary Material). The particular case of a real transition followed by a leapfrog transition, that traces a line in the 3D structure, is absorbed in one of these planes. In this sense, the anatomy of three-photon correlations is captured by the leapfrog planes and therefore remains relatively simple to comprehend.

4. Theory of Frequency-Resolved N-Photon Correlations

The correlations between N photons detected in as many (possibly degenerate) frequency windows as required, without restricting ourselves to the peaks, can be computed exactly with the theory of frequency-resolved correlations of del Valle et al.[33] In this formalism, one computes correlations between N "sensors" (in the simplest case, each sensor is a 2LS), at the frequencies ω_k to be correlated. Sensors correlations are then computed in the limit of their vanishing coupling ϵ to the system (in this text, the

**ADVANCED
SCIENCE NEWS**

www.advancedsciencenews.com

LASER
&PHOTONICS
REVIEWS

www.lpr-journal.org

resonantly fluorescing 2LS). The Hamiltonian describing such a coupling for the problem at hand is

$$H_{\xi_k} = \tilde{\omega}_k \xi_k^\dagger \xi_k + \epsilon \left(\sigma^\dagger \xi_k + \xi_k^\dagger \sigma \right), \tag{7}$$

where ξ_k is the annihilation operator of the kth sensor and $\tilde{\omega}_k = \omega_k - \omega_L$ is the detuning between the sensor and the driving laser. The spectral width of the filters enters in the formalism as the sensors decay rate Γ_k. The complete master equation of the 2LS supplemented with the set of sensors then reads

$$\partial_t \rho = i \left[\rho, H_\sigma + H_\xi \right] + \frac{\gamma_\sigma}{2} \mathcal{L}_\sigma \rho + \frac{1}{2} \mathcal{L}_\xi \rho, \tag{8}$$

where $H_\xi \equiv \sum_k H_{\xi_k}$ and $\mathcal{L}_\xi \rho \equiv \sum_k \Gamma_k \mathcal{L}_{\xi_k} \rho$, with the summation over as many sensors as required for the order of the correlation (N sensors for $g^{(N)}$). The two-photon (Fig. 1) and three-photon (Fig. 2) frequency-resolved correlations are thus computed as:

$$g_\Gamma^{(2)}(\tilde{\omega}_1, \tilde{\omega}_2) = \frac{\langle \xi_1^\dagger(\tilde{\omega}_1) \xi_2^\dagger(\tilde{\omega}_2) \xi_2(\tilde{\omega}_2) \xi_1(\tilde{\omega}_1) \rangle}{\langle \xi_1^\dagger(\tilde{\omega}_1) \xi_1(\tilde{\omega}_1) \rangle \langle \xi_2^\dagger(\tilde{\omega}_2) \xi_2(\tilde{\omega}_2) \rangle}, \tag{9a}$$

$$g_\Gamma^{(3)}(\tilde{\omega}_1, \tilde{\omega}_2, \tilde{\omega}_3) =$$

$$\frac{\langle \xi_1^\dagger(\tilde{\omega}_1) \xi_2^\dagger(\tilde{\omega}_2) \xi_3^\dagger(\tilde{\omega}_3) \xi_3(\tilde{\omega}_3) \xi_2(\tilde{\omega}_2) \xi_1(\tilde{\omega}_1) \rangle}{\langle \xi_1^\dagger(\tilde{\omega}_1) \xi_1(\tilde{\omega}_1) \rangle \langle \xi_2^\dagger(\tilde{\omega}_2) \xi_2(\tilde{\omega}_2) \rangle \langle \xi_3^\dagger(\tilde{\omega}_3) \xi_3(\tilde{\omega}_3) \rangle}, \tag{9b}$$

with an obvious generalization to higher orders. We have assumed for brevity only the case where all the filters have the same linewidth, although one can further enhance the correlations by optimizing the filters linewidths to match the width of the selected resonances. The case of different filter linewidths is further discussed in Ref. [39] and one can therefore consider in the following that there is still room for further improvement. Importantly, the normalization cancels the ϵ coupling, so that the result is a fundamental property of the system, only dependent on the filter linewidths—as is mandatory from the time-energy uncertainty—but otherwise independent from detectors efficiencies, coupling strengths, time of acquisition, etc.

A particular case of interest is the autocorrelation $g_\Gamma^{(N)}(\tilde{\omega})$ when all the frequencies are degenerate, $\tilde{\omega}_1 = \cdots = \tilde{\omega}_N$. This corresponds to the correlations, at various orders, of the light passing through a single filter. The cases up to fourth order as computed with the sensors technique are shown in **Fig. 3**. Panel (b) confirms the known results obtained in the literature[23,26,27] of antibunching for the side peaks, and also of bunching for the main peak ($g_\Gamma^{(2)}(\tilde{\omega} = 0) \approx 1.05$ with our parameters, see caption). Strikingly in the latter case, it is revealed that, in the full picture, this bunching actually sits in a local minimum and that although the central peak is indeed bunched, this comes in a region of suppressed bunching, as shown in the inset of Fig. 3(b) (zooming in the area indicated by the arrow). This feature is not fully conveyed by the dressed-atom picture. The most notable feature, however, is one that remained unnoticed until recently:[34] the two strong resonances that sit between the peaks. These are the leapfrog correlations. Similar results are generalized when turning to higher orders, as shown in panels (c) (three photons) and (d) (four photons). While the correlations of the peaks retain the same qualitative behaviours, new features thus appear away from the peaks,
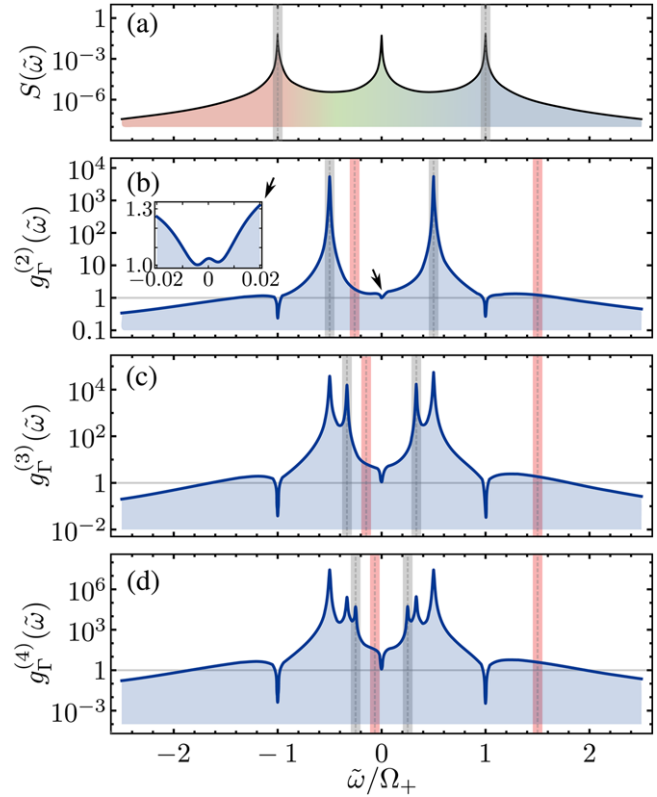
Figure 3. (Color online). Correlations between bundles of N photons. (a) Photoluminescence spectrum of the Mollow triplet, with the configuration of filters that has been proposed for single photon heralding in Ref. [27], namely, filtering the two side peaks. (b–d) 2, 3 and 4-photon autocorrelation spectrum. The resonances in the photon correlations reveal the frequencies where the same type of heralding but for N-photon bundles can be achieved. Such frequencies, shown here in gray, are given by $\tilde{\omega} = \pm\Omega_+/N$ at order N. In red are shown the even better configurations where the heralding does not involve any transition through a real state. The inset in Panel (b) shows a zoom of the correlations nearby the central peak, marked by an arrow, revealing bunching to sit on a local minimum. The decay rate of the 2LS sets the unit, the splitting of the triplet is set to $\Omega_+ = 300\gamma_\sigma$, the sensors linewidth to $\Gamma = 2\gamma_\sigma$, and the detuning between the laser and the 2LS to $\tilde{\omega}_\sigma = 200\gamma_\sigma$.

associated to the leapfrog transitions, successively captured by increasing the order of the correlations. These resonances, at $\pm\Omega_+/N$, pile up toward the central peak, and become increasingly difficult to access individually, as however can be expected from such strongly quantum objects involving a large number of particles.

While these cuts in the Nth-order correlation spectrum are useful and will be later referred to again—being so-closely connected to degenerate bundles—they provide a very simplified account of the structure of the correlations at the N-photon level. The case for $N = 3$ photons, displayed in Fig. 2(b) in two planes that intersect the full 3D spectrum, provides the full picture at this order, on the basis of which one can best exploit the photon emission. We will not discuss the antibunching patterns, whose intersections in the density plot produce in addition to straight lines, also a circular shape that is still of unclear physical origin but is not relevant for the points of this text. We will

**ADVANCED
SCIENCE NEWS**

www.advancedsciencenews.com

LASER
& PHOTONICS
REVIEWS

www.lpr-journal.org

now discuss how intercepting the red superbunching lines in the general three-dimensional space, that originate from the leapfrog planes in panels (b–e) of Fig. 2, allows to design a new family of heralded N-photon emitters.

5. Sources of Heralded Photons

With the formalism introduced in previous Section, it is straightforward to compute the exact frequency-resolved peak-peak correlations studied by Ulhad et al.[27] This includes their time-resolved version, beyond the coincidences that we have considered so far. The theory then needs to take proper care of time-ordering, which is however easily achieved with the sensors technique. The procedure to follow is presented in Ref. [33] and the underlying theory is detailed in its supplementary material. Since we consider here a system in its steady state, only relative time differences $\tau \equiv t_2 - t_1$ are of interest. Some frequency- and time-resolved correlations for the Mollow triplet are shown in **Fig.** 4(a), at both resonance (blue curves) and with a detuning between the 2LS and the laser frequencies (red curves). We compare the exact (solid) and approximated (dashed) solutions, obtained through the sensing formalism and the earlier theories, respectively. There is an excellent qualitative if not quantitative agreement. In the case of laser detuning, the asymmetric shape lends itself to heralding purposes, whereby detection of a photon from the high-energy peak correlates strongly with the detection of another photon from the low-energy peak.

The great advantage of the theory of frequency-resolved photon correlations[33] is that it also allows to compute exactly correlations in more general configurations than those restricted to the peaks. For instance, correlating the photons emitted by the leapfrog processes, by filtering at the corresponding frequencies, one gets the correlation function shown in Fig. 4(b), with several notable features, all in line with the quantum nature of these transitions. Namely, the correlations 1) are much stronger (about 50 times larger) than those of the photons emitted through real states, as shown in panel (a), 2) they have smaller correlation time (and thus yield better time resolutions), 3) they do not depend much on detuning, 4) they do not depend much on the choice of configuration (degenerate bundles or not) and 5) they are symmetric in time. Note that symmetric correlations are not detrimental for heralding, as the instantaneous character of the emission allows to delay one channel and thus keep the other as the heralding one. One obvious drawback of such strongly-correlated emission is the much reduced signal, since the collection is made away from the peaks. While there are ways to circumvent this limitation, for instance by Purcell enhancing them with a cavity of matching frequency,[35,43,44] we will remain here at the level of describing the naked correlations. Now that we have shown the new perspectives opened by the leapfrog process at the two-photon level, we focus on more innovative aspects.

6. Sources of Heralded Bundles

The powerful dressed-atom picture allows a straightforward generalization of the heralding discussed in the previous Section. One can contemplate the configuration where a photon heralds
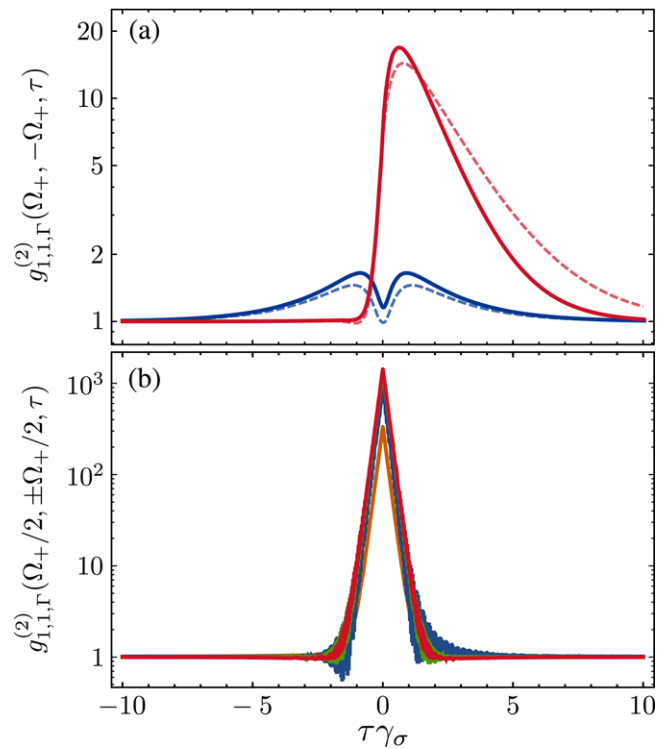
Figure 4. (Color online). Filtered single-photon correlations from the emission of, (a) the opposite sidebands, and, (b) the two-photon leapfrogs. Panel (a) shows the exact behaviour at resonance (solid blue) and with detuning (solid red), and compares it with the approximated expressions given in Ref. [26], shown as dashed blue and dashed red, respectively. Panel (b) shows the filtered correlations from the same two-photon leapfrog (shown in red at resonance and in green with detuning) and from the leapfrogs at opposite sides of the central peak (shown in orange at resonance and in blue with detuning). The curves essentially overlap, meaning that, thanks to the nature of the leapfrog transitions, the choice of configuration in which a two-photon bundle heralds another one is not very important. The decay rate of the 2LS sets the unit, $\Omega_+ = 300\gamma_\sigma$, $\Gamma = 5\gamma_\sigma$ and in the cases with detuning, $\tilde{\omega}_\sigma = 200\gamma_\sigma$.

a bundle in the radiative cascade down the ladder, as shown in case i of **Fig.** 5(c). This is the same idea as Ulhaq et al.'s heralding a single-photon, but now heralding a bundle instead. Even better, however, is to consider a three-photon leapfrog where all photons are virtual, and use one of them to herald the other two, a sketched in case ii. Conveniently, one can use the heralding photon to have a different energy from the two other ones, that can be degenerate. One needs a careful analysis, however, since there is room for subtleties in a relaxation process that starts to be complex. As an illustration, case ii, that has no real photons, has in fact the same distribution of photon frequencies as case i, that transits via a real state. The difference is the initial and final states, $|-\rangle \rightarrow |+\rangle \rightrightarrows |-\rangle$ and $|+\rangle \overset{3}{\rightrightarrows} |+\rangle$. For this reason, case ii turns out to be suppressed as a three-photon leapfrog process, as revealed by the exact calculation. One needs instead to find a case such as iii that suffers no such interference with another relaxation in the ladder intersecting with a real state. A quantitative analysis is thus required, and the theory of frequency-resolved photon correlations[33] here again allows us to easily tackle this

**ADVANCED
SCIENCE NEWS**

www.advancedsciencenews.com

LASER
&PHOTONICS
REVIEWS

www.lpr-journal.org
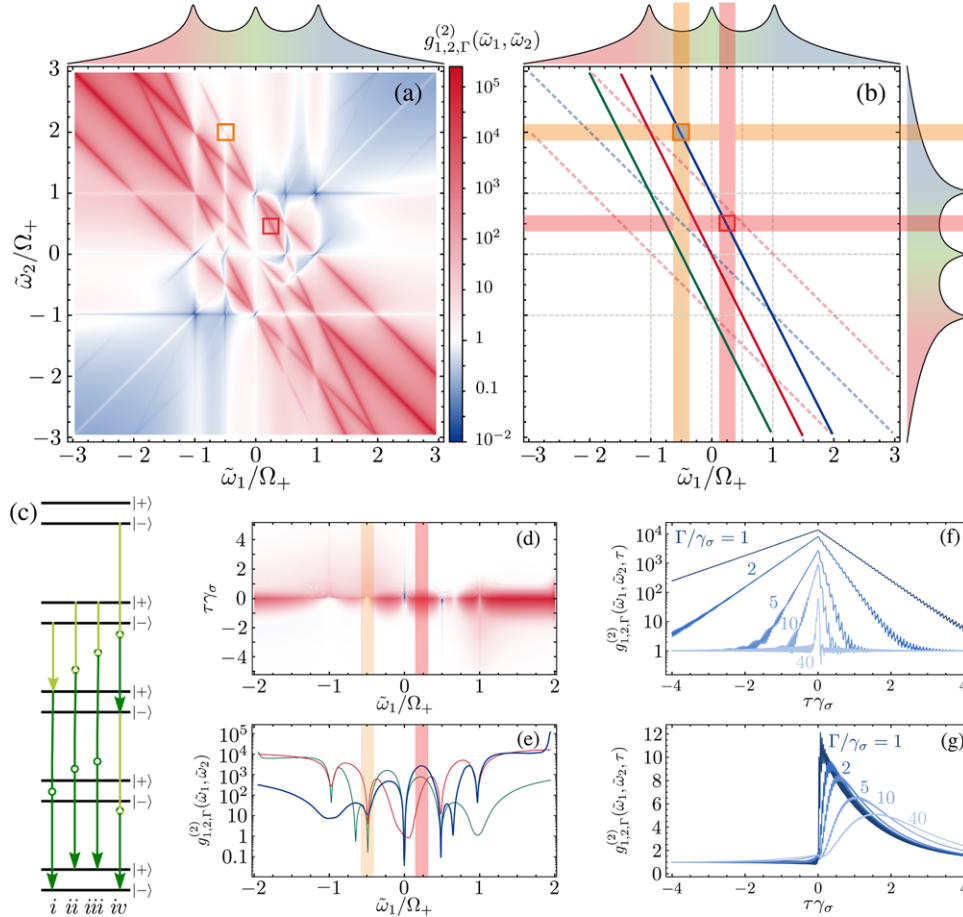
Figure 5. (Color online). Correlations between a single photon and a bundle of two photons. Panel (a) displays the full correlation spectrum $g_{1,2,\Gamma}^{(2)}(\tilde{\omega}_1, \tilde{\omega}_2)$ between a single photon with frequency $\tilde{\omega}_2$ and a bundle of two photons, each with frequency $\tilde{\omega}_1$. The antidiagonals of superbunching are shown in Panel (b): the dashed lines correspond to the transitions $\tilde{\omega}_1 + \tilde{\omega}_2 = \Delta$, whereas the solid lines correspond to the transitions $2\tilde{\omega}_1 + \tilde{\omega}_2 = \Delta$. The latter are shown in the ladder of Panel (c) as cases i–iii, where the dark green arrows represent the two-photon bundles and the light green arrows the single photon. Panel (d) shows the τ-dynamics along the blue antidiagonal of panel (b), while panel (e) shows the correlation intensities for all the solid antidiagonals, with the same color code. Panels (f) and (g) show the time-correlations measured at the frequencies specified by the red and orange filters. Although the correlations in panel (g) have the λ-shape commonly associated to photon heralding, the correlations in panel (f) are much stronger. Note that while the correlations captured by the orange filters, with the two-photon bundle emitted at $\tilde{\omega}_1 = -\Omega_+/2$, are bunched, they actually correspond to a local minimum, as seen in panel (e) for the blue line. The global maximum, instead, lies at a frequency with no particular attribute that one would not a priori target without the knowledge of the photon-bundle correlation spectrum. Its frequency is one captured by the red filters. The triplet splitting is $\Omega_+ = 300\gamma_\sigma$, the detuning between the laser and the 2LS is $\tilde{\omega}_\sigma = 200\gamma_\sigma$ and the spectral width of the sensors is $\Gamma = 5\gamma_\sigma$, except in panels (f) and (g), where the filter size is specified for each curve.

problem. The relevant correlation is the one that generalizes Eq. (9a) to the N-th order correlation function of N bundles, with each of them—detected at frequency $\tilde{\omega}_\mu$—being composed of n_μ photons:

$$g_{n_1,\cdots,n_N,\Gamma}^{(N)}(\tilde{\omega}_1,\ldots,\tilde{\omega}_N) \equiv \frac{\langle : \Pi_{\mu=1}^N \xi_\mu^{\dagger\,n_\mu}(\tilde{\omega}_\mu) \xi_\mu^{n_\mu}(\tilde{\omega}_\mu) : \rangle}{\Pi_{\mu=1}^N \langle \xi_\mu^{\dagger\,n_\mu}(\tilde{\omega}_\mu) \xi_\mu^{n_\mu}(\tilde{\omega}_\mu) \rangle},$$

(10)

where ":" indicates normal ordering, a necessary requirement when two (or more) of the sensors have the same frequency. With this notation, Eq. (9a) is the particular case with $N = 2$ and $n_1 = n_2 = 1$. For the simplest extension to Ulhaq *et al.*'s

paradigm, that is, one photon heralding a two-photon bundle, one therefore deals with

$$g_{1,2,\Gamma}^{(2)}(\tilde{\omega}_1,\tilde{\omega}_2) = \frac{\langle : \xi_1^\dagger(\tilde{\omega}_1) \xi_2^{\dagger\,2}(\tilde{\omega}_2) \xi_2^2(\tilde{\omega}_2) \xi_1(\tilde{\omega}_2) : \rangle}{\langle \xi_1^\dagger(\tilde{\omega}_1) \xi_1(\tilde{\omega}_1) \rangle \langle \xi_2^{\dagger\,2}(\tilde{\omega}_2) \xi_2^2(\tilde{\omega}_2) \rangle}.$$

(11)

Figure 5(a) shows this quantity computed for the Mollow triplet and, in (b), the mathematical structure of this photon-bundle correlation spectrum. The "heralding scenario" of one photon, of frequency $\tilde{\omega}_2$, announcing a two-photon bundle, made of photons of frequency $\tilde{\omega}_1$, follows from Eq. (5) with $N = 3$ and $\tilde{\omega}_3 = \tilde{\omega}_1$, resulting in correlations for $g_{1,2}^{(2)}$ when the condition

$$2\tilde{\omega}_1 + \tilde{\omega}_2 = \Delta$$

(12)

**ADVANCED
SCIENCE NEWS**

www.advancedsciencenews.com

LASER
&PHOTONICS
REVIEWS

www.lpr-journal.org

is met, with, as before, $\Delta = 0$ or $\pm\Omega_+$. These yield the steeper lines in Fig. 5(a), reproduced as solid lines in (b). They correspond to transitions of the type i–iii in the ladder of panel (c). The antidiagonals, with the same strength than the three-photon bundles, correspond to transitions of the type iv in panel (c), namely, a two two-photon bundle cascade, transiting by an intermediate real state. Two photons from different leapfrogs can have the same frequency, allowing for their detection as an apparent bundle, although actually emanating from different bundles, related by a cascade through a real state. In this case, any of the other photon can be detected as the heralder while the fourth photon is discarded. Although we have shown previously that correlations that involve a real state are weaker than those that only involve virtual states, this is when comparing processes of the same order, i.e., with the same number of photons. Here the two two-photon bundle transition involves a cascade through a real state but is otherwise composed of (two) second-order processes, while the three-photon bundle that does not involve a real state, is a third-order process. All this considered, the exact computation shows that these processes result in correlations of similar strength in the correlation spectrum, as seen in Fig. 5. This could be generalized although the combinatorial explosion of different ways in which N photons can be correlated at the same order would make such a discussion difficult, and we believe that the three-photon case is illustrative of the overall situation. Therefore, coming back to the three-photon bundle, specified by Eq. (12), we show in Fig. 5(d) the photon-bundle correlations $g_{1,2,\Gamma}^{(2)}(\tau)$ along the leapfrog transitions. We highlight the case $|+\rangle \rightrightarrows |-\rangle$ (blue line in panel (b)), the results being similar for other leapfrogs. The density plot allows to spot where the photon-bundle correlations are the strongest. One sees, as expected, that correlations are smothered when intersecting a real state, even exhibiting antibunching instead of superbunching for the cases $\tilde{\omega}_1/\Omega_+ = 0$ (intersecting with the central peak) and $\tilde{\omega}_1/\Omega_+ = \pm 1/2$ (leapfrogs). Since, by the nature of the leapfrog correlations, they are fairly symmetric in τ and maximum at zero, we can identify the optimum as the local maximum nearby the peaks of $g_{1,2}^{(2)}(\tilde{\omega}_1, (\Delta - \tilde{\omega}_1)/2)$, shown in Fig. 5(e). It lies in good approximation between the two depletions in correlations already described. The correlations in time there for various filter sizes are shown in panel (f), reproducing in this photon-bundle scenario the same phenomenology as the photon-photon correlations shown in Fig. 4(b). The oscillations that are observed in time are due to the spectral width of the sensors, which detects photon from transitions other than the N-photon leapfrog, causing interferences. Such an oscillatory behaviour can be reduced either by turning to a triplet with a larger splitting, in which the emission from different transitions are further apart, or by using a smaller filter width. The photon-bundle correlations display strikingly the same phenomenology as the photon-photon case of Fig. 4. Namely, they are completely symmetric in time, regardless of the size of the bundle, i.e., the cascade emission of N-photon bundles from opposite sides of the Mollow triplet does not have a preferential order. The temporal symmetry can be broken by involving a real transition and detuning the laser from the 2LS. To complete the analogy with Fig. 4, we also show in panel (g) the transition that involves a real state transition for the photon heralding the bundle. In this case, the correlation profile shown in (g) is obtained, in clear analogy
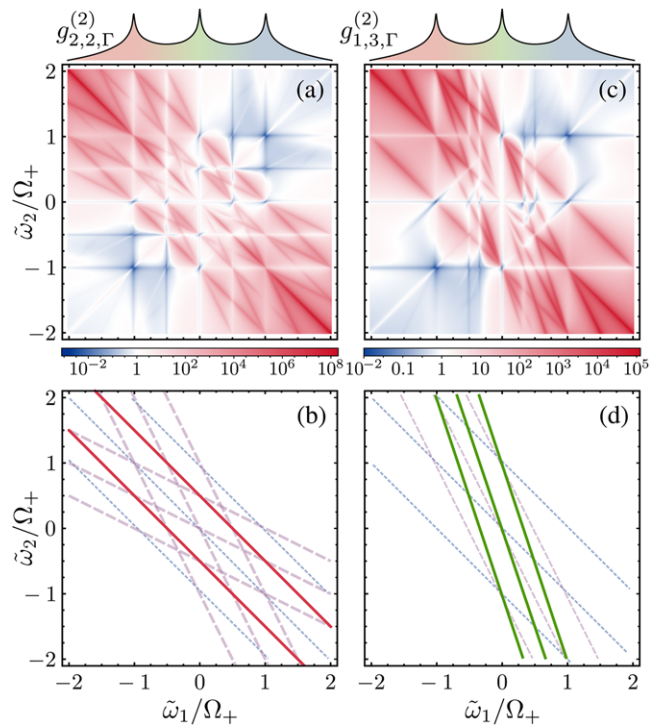
Figure 6. (Color online). Correlations involving four photons. (a) Landscape of correlations between two-photon bundles as given by $g_{2,2,\Gamma}^{(2)}(\tilde{\omega}_1, \tilde{\omega}_2)$. (b) Mathematical structure of the correlations with transitions $\tilde{\omega}_1 + \tilde{\omega}_2 = \Delta$ (shown as dotted blue lines), $\tilde{\omega}_1 + 2\tilde{\omega}_2 = \Delta$ and $2\tilde{\omega}_1 + \tilde{\omega}_2 = \Delta$ (dashed purple), and $2\tilde{\omega}_1 + 2\tilde{\omega}_2 = \Delta$ (solid red), where $\Delta = -\Omega_+, 0, \Omega_+$. (c) Correlations between a three-photon bundle, in which each photon has frequency $\tilde{\omega}_1$, and a single photon with frequency $\tilde{\omega}_2$. (d) Mathematical structure of the correlations with transitions $3\tilde{\omega}_1 + \tilde{\omega}_2 = \Delta$ (shown in solid green) and the transitions described in (b). The decay rate of the 2LS sets the unit, $\Omega_+ = 300\gamma_\sigma$, $\tilde{\omega}_\sigma = 200\gamma_\sigma$ and $\Gamma = 5\gamma_\sigma$.

of Fig. 4(a). So one has these two options of heralding a bundle with a photon, would one scenario be better suited than the other. The Mollow triplet can thus be turned into a tuneable and versatile source of N-photon bundles simply by filtering its emission at the adequate spectral windows.

This physics can be generalized, in principle, to any higher order. Of course, an actual experiment measuring such correlations would be increasingly challenging. Still, for the sake of illustration, we now quickly address the case of four-photon bundles (and parenthetically the general case of N-photon bundles). The leapfrog are then hyperplanes of dimension 3 (N) in an hyperspace of dimension 4 ($N+1$), which we shall not attempt to represent. Instead, we show the two-bundle correlation spectra, in **Fig. 6**. When correlating two bundles of two-photons each, we recover a landscape fairly similar to that of Fig. 1. When correlating a photon with the rest of the bundle, we turn to the heralding scenario. The number of possibilities is that given by the integer partition of 3 (N), which is conveniently represented as Young tableaux, whose number of rows is the order of the correlation, and with each entry providing the composition of the correlated bundles:

1. ☐ for $g^{(4)}_{1,1,1,1}$, the standard Glauber correlator $g^{(4)}$,

2. ⊞ for $g^{(2)}_{2,2}$, shown in Fig. 6(a),

3. ⊞☐ for $g^{(2)}_{1,3}$, shown in Fig. 6(b),

4. ⊟ for $g^{(3)}_{1,1,2}$.
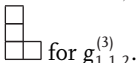
The non-partitioned case ☐☐☐☐ does not lead to a correlator (it could be understood as normal luminescence). Maybe the most useful configuration is ⊞···☐☐, with a single photon heralding a N-photon bundle. The case of one photon heralding a 3-photon bundle lies on any of the corresponding leapfrogs shown as the steepest lines in Fig. 6(b), with general equation $N\tilde{\omega}_1 + \tilde{\omega}_2 = \Delta$ (the case $N = 3$ is the one shown in the figure). While it might be less obvious that other configurations could also be useful, it would not be surprising on the other hand that the need could arise with the boom of quantum technologies. It seems that, in such a case, the Mollow triplet can serve as a universal photon-emitter, able to deliver any requested configuration, e.g., distributing ten photons in a five channel input with two single photons, two two-photon bundles and a four-photon bundle:

$$ \tag{13} $$

Would such a profile be required to feed a quantum gate, it is a small technical matter to identify which spectral windows would capture this configuration and filter it out from the total luminescence. Once again, here we do not address specifically the issue of the signal, but only point to the structure of the photon correlations that reside in the Mollow triplet. We highlight as well that, in addition to feeding boson sampling devices, the very combinatorial nature of the emission could allow to test quantum supremacy through photon detection only, without the need of interposing a complex Galton board of optical beam-splitters. Whatever its actual use for practical applications, it is clear that the Mollow triplet overflows with possibilities, so characteristic of strongly-correlated quantum emission.

7. Conclusions and Perspectives

We have shown that the Mollow triplet is a treasure trove of quantum correlations, at all orders and not limited to dressed-state transitions. Specifically, we have shown—based on both qualitative arguments rooted in the structure of the dressed-atom ladder and exact computations made possible by a recent theory of frequency-resolved N-photon correlations—that the emission from the Mollow triplet exhibits its richest potential when dealing with leapfrog transitions, i.e., processes that occur through virtual photons, endowing them with much stronger correlations.

While the focus of photon correlations from the Mollow triplet has been on correlations between two photons from the peaks, following the picture of a radiative cascade between dressed states, our results should encourage the study of correlations from photons away from the spectral peaks, where the emission from a Mollow triplet at the appropriate frequencies can be used as a heralded source of N-photon bundles or, taking full advantage of the scheme, any customisable configuration of photons. At an applied level, including with the use of cavities to Purcell enhance these transitions and turn the virtual processes into real ones, this should allow to develop new types of quantum emitters, of interest for instance for multiphoton quantum spectroscopy,[45] or to deepen the tests of nonlocality and quantum interferences between correlated photons.[40] Our result only scratches the surface of the possibilities that reside in the Mollow triplet, which should be of interest as programmable quantum inputs for future photonic applications.

Conflict of Interest

The authors have declared no conflict of interest.

[1] W. Vogel and D. G. Welsch, *Quantum Optics* (Wiley-VCH, 3, 2006).

[2] H. J. Carmichael and D. F. Walls, *J. Phys. B.: At. Mol. Phys.* **9**, 1199 (1976).

[3] H. J. Kimble, M. Dagenais, and L. Mandel, *Phys. Rev. Lett.* **39**, 691 (1977).

[4] W. Heitler, *The Quantum Theory of Radiation* (Oxford University Press, 1944).

[5] J. C. López Carreño, C. Sánchez Muñoz, E. del Valle, and F. P. Laussy, *Phys. Rev. A* **94**, 063826 (2016).

[6] I. Aharonovich, D. Englund, and M. Toth, *Nat. Photon.* **10**, 631 (2016).

[7] B. R. Mollow, *Phys. Rev.* **188**, 1969 (1969).

[8] F. Schuda, C. R. S. Jr, and M. Hercher, *J. Phys. B.: At. Mol. Phys.* **7**, L198 (1974).

[9] C. H. Keitel, P. L. Knight, L. M. Narducci, and M. O. Scully, *Opt. Commun.* **118**, 143 (1995).

[10] M. Bienert, W. Merkel, and G. Morigi, *Phys. Rev. A* **69**, 013405 (2004).

[11] M. Bienert, J. M. Torres, S. Zippilli, and G. Morigi, *Phys. Rev. A* **76**, 013410 (2007).

[12] E. B. Flagg, A. Muller, J. W. Robertson, S. Founta, D. G. Deppe, M. Xiao, W. Ma, G. J. Salamo, and C. K. Shih, *Nat. Phys.* **5**, 203 (2009).

[13] O. Astafiev, A. M. Zagoskin, A. A. A. Jr., Y. A. Pashkin, T. Yamamoto, K. Inomata, Y. Nakamura, and J. S. Tsai, *Science* **327**, 840 (2010).

[14] M. N. Makhonin, J. E. Dixon, R. J. Coles, B. Royall, I. J. Luxmoore, E. Clarke, M. Hugues, M. S. Skolnick, and A. M. Fox, *Nano Lett.* **14**, 6997 (2014).

[15] D. M. Toyli, A. W. Eddins, S. Boutin, S. Puri, D. Hover, V. Bolkhovsky, W. D. Oliver, A. Blais, and I. Siddiqi, *Phys. Rev. X* **6**, 031004 (2016).

[16] S. Unsleber, Y. M. He, S. Gerhardt, S. Maier, C. Y. Lu, J. W. Pan, N. Gregersen, M. Kamp, C. Schneider, and S. Höfling, *Opt. Express* **24**, 8539 (2016).

[17] K. Lagoudakis, K. Fischer, T. Sarmiento, P. McMahon, M. Radulaski, J. Zhang, Y. Kelaita, C. Dory, K. Müller, and J. Vučković, *Phys. Rev. Lett.* **118**, 013602 (2017).

[18] Y. Zhou, A. Rasmita, K. Li, Q. Xiong, I. Aharonovich, and W. Gao, *Nat. Comm.* **8**, 14451 (2017).

[19] C. N. Cohen-Tannoudji and S. Reynaud, *J. Phys. B.: At. Mol. Phys.* **10**, 345 (1977).

[20] S. Reynaud, *Annales de Physique* **8**, 315 (1983).

[21] P. A. Apanasevich and S. Y. Kilin, *J. Phys. B.: At. Mol. Phys.* **12**, L83 (1979).

[22] C. Cohen-Tannoudji and S. Reynaud, *Phil. Trans. R. Soc. Lond. A* **293**, 223 (1979).

[23] A. Aspect, G. Roger, S. Reynaud, J. Dalibard, and C. Cohen-Tannoudji, *Phys. Rev. Lett.* **45**, 617 (1980).

[24] A. Al-Hilfy and R. Loudon, *J. Phys. B.: At. Mol. Phys.* **18**, 3697 (1985).

[25] C. A. Schrama, G. Nienhuis, H. A. Dijkerman, C. Steijsiger, and H. G. M. Heideman, *Phys. Rev. Lett.* **67** (1991).

[26] C. A. Schrama, G. Nienhuis, H. A. Dijkerman, C. Steijsiger, and H. G. M. Heideman, *Phys. Rev. A* **45**, 8045 (1992).

[27] A. Ulhaq, S. Weiler, S. M. Ulrich, R. Roßbach, M. Jetter, and P. Michler, *Nat. Photon.* **6**, 238 (2012).

[28] S. L. Portalupi, M. Widmann, C. Nawrath, M. Jetter, P. Michler, J. Wrachtrup, and I. Gerhardt, *Nat. Comm.* **7**, 13632 (2016).

[29] H. F. Arnoldus and G. Nienhuis, *J. Phys. B.: At. Mol. Phys.* **17**, 963 (1984).

[30] L. Knöll, G. Weber, and T. Schafer, *J. Phys. B.: At. Mol. Phys.* **17**, 4861 (1984).

[31] G. Nienhuis, *Phys. Rev. A* **47**, 510 (1993).

[32] L. Knöll and G. Weber, *J. Phys. B.: At. Mol. Phys.* **19**, 2817 (1986).

[33] E. del Valle, A. González-Tudela, F. P. Laussy, C. Tejedor, and M. J. Hartmann, *Phys. Rev. Lett.* **109**, 183601 (2012).

[34] A. González-Tudela, F. P. Laussy, C. Tejedor, M. J. Hartmann, and E. del Valle, *New J. Phys.* **15**, 033036 (2013).

[35] E. del Valle, *New J. Phys.* **15**, 025019 (2013).

[36] C. Sánchez Muñoz, E. del Valle, C. Tejedor, and F. Laussy, *Phys. Rev. A* **90**, 052111 (2014).

[37] M. Peiris, B. Petrak, K. Konthasinghe, Y. Yu, Z. C. Niu, and A. Muller, *Phys. Rev. B* **91**, 195125 (2015).

[38] E. del Valle, A. González-Tudela, E. Cancellieri, F. P. Laussy, and C. Tejedor, *New J. Phys.* **13**, 113014 (2011).

[39] A. González-Tudela, E. del Valle, and F. P. Laussy, *Phys. Rev. A* **91**, 043807 (2015).

[40] M. Peiris, K. Konthasinghe, and A. Muller, *Phys. Rev. Lett.* **118**, 030501 (2017).

[41] R. J. Glauber, *Phys. Rev. Lett.* **10**, 84 (1963).

[42] F. P. Laussy, E. del Valle, M. Schrapp, A. Laucht, and J. J. Finley, *J. Nanophoton.* **6**, 061803 (2012).

[43] C. Sánchez Muñoz, E. del Valle, A. González-Tudela, K. Müller, S. Lichtmannecker, M. Kaniber, C. Tejedor, J. Finley, and F. Laussy, *Nat. Photon.* **8**, 550 (2014).

[44] C. Sánchez Muñoz, F. P. Laussy, C. Tejedor, and E. del Valle, *New J. Phys.* **17**, 123021 (2015).

[45] J. C. López Carreño, C. Sánchez Muñoz, D. Sanvitto, E. del Valle, and F. P. Laussy, *Phys. Rev. Lett.* **115**, 196402 (2015).